

# ACTIVE BIOMONITORING OF ATMOSPHERIC DEPOSITION OF METAL/METALLOIDS USING *RAMALINA SINENSIS* TRANSPLANTS IN URBAN, SUBURBAN AND RURAL MOUNTAIN AREAS OF BAODING AND SHIJIAZHUANG, NORTH CHINA

ZHU, X. H.<sup>1</sup> – LI, X. J.<sup>2</sup> – WU, Q. F.<sup>1</sup> – ZHAO, R. K.<sup>2</sup> – GAO, J.<sup>1,3</sup> – XU, P.<sup>1,3</sup> – WANG, W. J.<sup>1</sup> – CHEN, C.<sup>2</sup> – ZHAO, L. C.<sup>2</sup> – LIU, H. J.<sup>1\*</sup>

<sup>1</sup>*School of Life Sciences, Institute of Life Science and Green Development, Hebei University, Baoding, Hebei Province, China*  
(e-mail: xhzhu2023@163.com; wqf45@126.com; 1182212156@qq.com; pxu2000@163.com; liuhuajie@hbu.edu.cn)

<sup>2</sup>*Hebei Key Laboratory of Mineral Resources and Ecological Environment Monitoring, Hebei Research Center for Geoanalysis, Baoding, Hebei Province, China*  
(e-mail: 1056816294@qq.com; zrkzzl75@163.com; hello-juan@163.com; 6539149@qq.com; zhao.l.c@163.com)

<sup>3</sup>*Key Laboratory of Microbial Diversity Research and Application of Hebei Province, Research Center for Microbial Breeding and Conservation Engineering, Baoding, Hebei Province, China*

\*Corresponding author  
e-mail: liuhuajie@hbu.edu.cn

(Received 6<sup>th</sup> Feb 2025; accepted 24<sup>th</sup> Mar 2025)

**Abstract.** Baoding and Shijiazhuang are key areas of air pollution in North China, especially in the winter heating period. However, atmospheric deposition levels of metal/metalloids across different ecotopes in these cities need further investigation. During the winter heating period, from November 2018 to March 2019, we exposed the lichen *Ramalina sinensis* (RSI) to three ecotopes (urban, suburban, and rural mountain) in both cities for 140 days and measured concentrations of 55 elements in both exposed and unexposed RSI samples using inductively coupled plasma mass spectrometry (ICP-MS). The results show that the concentrations of potassium (K) and phosphorus (P) in the exposed samples were lower than those in the unexposed samples, suggesting nutrient loss in RSI due to air pollution in the exposure areas. For most of the studied elements (48 out of 50), its concentrations were significantly higher in the exposed samples compared to the unexposed ones but were not different between cities and among ecotopes. Among the 50 elements, chromium (Cr) and antimony (Sb) exhibited moderate bioaccumulation, primarily linked to industrial and traffic activities, while the bioaccumulation of the other 48 elements was low and attributed to atmospheric-crustal sources. These findings suggest that air pollution in the exposure areas is not severe and is primarily influenced by non-point pollution sources during the exposure period. Increased attention should be given to the emissions from industrial and traffic activities, particularly those associated with Cr and Sb.

**Keywords:** *urbs, suburbs, atmospheric deposition, air pollution, lichen biomonitoring*

## Introduction

In recent decades, urban agglomerations in North China had high concentration loading of atmospheric heavy metals in aerosols and great atmospheric metal/metalloid deposition flux due to the dual effects of local anthropogenic emissions from the North China Plain and dust transport from the arid/semi-arid regions of Northwest China (Wang et al., 2019). This is especially true for the urban agglomerations in the Piedmont Plain

of Taihang Mountains, where the atmospheric heavy metals/metalloid pollutants released in the plain were transported to the Taihang Mountains. Atmospheric deposition contributed 50-93% for As, Cd, Cr, Hg, Ni and Pb inputs in farmlands in China, highlighting strong negative impacts on human and ecosystem health in both urban and remote areas (Peng et al., 2019).

Baoding and Shijiazhuang are the key areas for the development of the persistent regional pollution events in North China in recent decades, especially in the winter heating period (Wang et al., 2018; Li et al., 2020). The ecotopes (urbs, suburbs, and rural mountains) in both cities are generally different in traffic and industrial intensity, biomass and coal combustion, and population density. However, atmospheric deposition of metal/metalloids is still poorly studied in ecotopes of Baoding and Shijiazhuang. This is because the conventional automated monitoring systems in the country generally detect the punctual concentrations of a limited number of contaminants/pollutants, such as atmospheric suspended particulate matters (PM<sub>2.5</sub> and PM<sub>10</sub>) and gases (NO<sub>x</sub>, SO<sub>2</sub>, O<sub>3</sub>, and CO etc.). Such monitoring systems are implemented in a limited number of sites and do not monitor atmospheric deposition of metal/metalloids.

Active biomonitoring technique using lichen transplants is a powerful tool for integrating atmospheric metal/metalloid deposition over a long period in large areas at low cost, and therefore it is an effective compensation for the conventional monitoring systems. In this technique, the lichens are generally taken from a “clean” site and exposed to the polluted sites, and element composition in lichen transplants before and after exposure are recorded (Brunialti and Frati, 2014; Abas, 2021). Lichens are an association of fungi and green algae/cyanobacteria. These organisms are highly dependent on atmospheric deposition of nutrients, and can accumulate the atmospheric pollutants in amounts exceeding their metabolic requirements (Abas, 2021). Metal concentrations in lichen transplants are positively correlated with those in the air, indicating that lichens are good active biomonitors for atmospheric element deposition (Paoli et al., 2018; Massimi et al., 2019).

Foliose lichens are preferred in active biomonitoring method due to their large surface area, which allows a high capacity of element uptake from the air (Abas, 2021). Among which, *Ramalina sinensis* (*RSI*; Fig. 1a) has been validated a good active biomonitor (Tumur et al., 2011; Sohrabi et al., 2021; Gao et al., 2022; Li et al., 2024). In addition, the other four foliose lichens have also been used as active biomonitors in Northern China, they are *Evernia mesomorpha* (Lin et al., 2024), *Xanthoparmelia camtschadalis* (Jia et al., 2020), *Flavopunctelia soredica* and *Rhizoplaca chrysoleuca* (Zhao et al., 2019).

We transplanted *RSI* (Fig. 1a) from a clean site to the three ecotopes (urbs, suburbs, and rural mountains) of Baoding and Shijiazhuang (Fig. 1b-d) in winter heating period. The unexposed and exposed concentrations for 55 elements were analyzed. These elements are Ag, Al, As, B, Ba, Be, Bi, Ca, Cd, Co, Cr, Cs, Cu, Fe, Ge, Hg, K, Li, Mg, Mn, Mo, Na, Nb, Ni, P, Pb, Rb, S, Sb, Se, Si, Sn, Sr, Th, Ti, Tl, U, V, and Zn, as well as 16 REEs (Sc, Y, La, Ce, Pr, Nd, Sm, Eu, Gd, Tb, Dy, Ho, Er, Tm, Yb, and Lu). Our purpose was to evaluate the differences in atmospheric deposition levels between cities and among ecotopes. This study is one of the few active lichen biomonitoring studies in China and also one of the studies involving the largest number of elements.

## Materials and methods

### Background area, sample collection and preparation

The background area is Saihanba Forest Farm, Hebei Province, North China (Fig. 1b). The climate, geology, and vegetation are detailed in our previous studies (Li et al., 2024; Lin et al., 2024). In short, Saihanba Forest Farm is a remote mountain forest ecosystem dominated by *Larix gmelinii* (Rupr.) Kuzen. and *Betula platyphylla* Suk with a forest coverage of 80%. The area is sparsely populated with few industrial and agricultural activities and low concentrations of atmospheric pollutants (PM<sub>2.5</sub>, PM<sub>10</sub> and SO<sub>2</sub>; Fig. 1e).

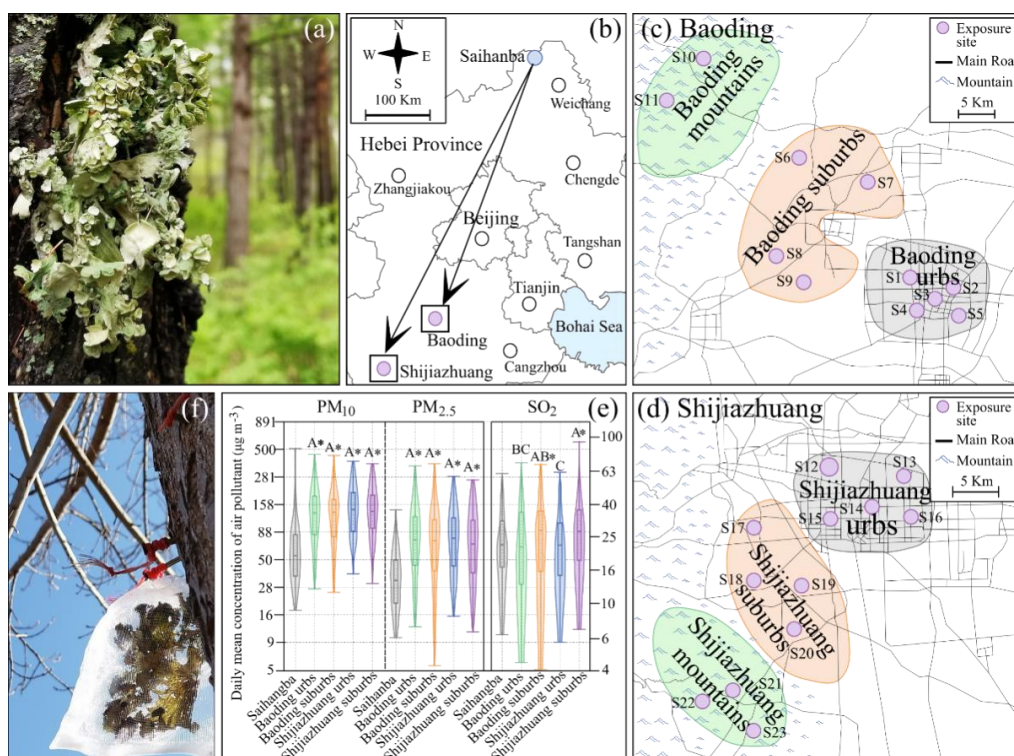


**Figure 1.** (a) *Ramalina sinensis* in the background area (Saihanba). (b) Location of Saihanba, Baoding and Shijiazhuang. (c) Selected ecotopes and exposure sites in Baoding. (d) Selected ecotopes and exposure sites in Shijiazhuang. (e) Box and violin plot of daily mean concentration of air pollutants in the background area, and urbs and suburbs of Baoding and Shijiazhuang during exposure period; A same letter denotes concentrations were not significantly different between the exposure areas. A “\*” denotes concentrations were significantly different between the background and exposure areas. Differences were tested by One-way ANOVA with a Turkey’s HSD test for multiple comparisons;  $\alpha = 0.05$ . Data sourced from the Baoding Meteorological Bureau of Hebei Province. (f) Exposed samples of *Ramalina sinensis*

We collected *RSI* samples on Oct. 30, 2018, within a site of 500×500 m<sup>2</sup> (42°14’N, 117°14’E), at an altitude of 1681-1700 m. The procedures of sample collection and preparation are detailed in our previous studies (Li et al., 2024; Lin et al., 2024), and have been adopted by many authors (Agnan et al., 2014; Klos et al., 2018; Dörter et al., 2020). In short, *RSI* thalli of 2-4 cm in size were randomly collected by hand from all aspects of tree barks at a height of 1-2 m from the ground. All samples were rinsed 3-5 times with

deionized water, each lasting for 5 s. Each sample was a composite sample consisting of 4-6 thalli (dry weight 4.0-6.0 g). We randomly selected 5 samples as control samples, and put the other samples into nylon bags for exposure. The procedures mentioned above can minimize the effects of collection height and collection aspects on the lichen element concentrations (Adams and Gottardo, 2012). The adoption of composite samples comprising thalli of similar size can minimize the effects of intra-species effects on lichen element concentrations (Zheng et al., 2023). Washing the samples can effectively lower the unexposed concentrations and their variability (Godinho et al., 2009; Kumari et al., 2024).

### ***Exposure area and sample exposure***

The exposure areas are located in Baoding and Shijiazhuang of Hebei Province, North China (*Fig. 1b*). Both cities were the key areas of development of persistent regional pollution events in northern China (Li et al., 2020). According to a study on the aerosol heavy metal contents in 44 cities in China before 2013, Shijiazhuang ranked in the bottom 1 in terms of Zn and V, in the bottom 3 in terms of Mn and Ni, and in the bottom 4 in terms of Cr and Pb (Duan and Tan, 2013). During 2013 to 2015, Baoding and Shijiazhuang were the cities that contributed the most to regional emissions of atmospheric suspended particulate matters among the southern cities of Hebei Province (Wang et al., 2018). Air quality is the worst in the winter heating period (Nov. 15-Mar. 15), in which the atmospheric pollutants often cross the Taihang Mountains, forming a continuous persistent haze from the North China Plain to the Shanxi Basins (Wang et al., 2018).

We selected six exposure areas in three different ecotopes of the two cities. Urbs of the two cities are located in the plain, surrounded by the dense highways, with a high population density and a certain degree of industrial activities. Suburbs of the two cities are located to the west of the urbs and are plains with the villages, roads, and agricultural and industrial sites. Rural mountains are located to the west of the suburbs, with a large number of shrubs and woodlands, moderate farmland, and sparse villages and roads. The traffic intensity and population density decrease from the urbs to suburbs to rural mountains. The industrial intensity is higher in the urbs and suburbs than that in the rural mountains.

In each exposure area, we selected 3-5 exposure sites with a minimum distance of 3-5 km (*Fig. 1c,d*). In each exposure site, we set 3-5 replicates, each replicate is a composite sample packaged into several nylon bags. Nylon bags containing *RSI* thalli were hung to the tree trunks at a height of 1.5-2.5 m for exposure (*Fig. 1f*).

*RSI* samples were exposed on Nov. 7-10, 2018, and recovered on Mar. 29-31, 2019 after exposure for 140 days. A total of 95 exposure samples in 23 exposure sites of 6 exposure areas were recovered (*Table 1*).

According to the data from Baoding Meteorological Bureau of Hebei Province, during the experiment period, concentrations of both  $PM_{10}$  and  $PM_{2.5}$  were higher in the exposure areas than those in the background area, and were not different between the two cities and between the urbs and suburbs. Concentration of  $SO_2$  in the background area was lower than that in the suburbs, but was similar to that in the urbs (One-way ANOVA with a Turkey's HSD test for multiple comparisons;  $\alpha = 0.05$ ; *Fig. 1e*). Data of air pollutants are lacking in the concerned rural mountains.

**Table 1.** Exposure area, exposure site, recovered sample, site weighting, and sampling site GPS coordinates (Weighting ensures equal exposure sites across all exposure areas)

Exposure area	Exposure site	Number of samples	Weighting value for each site	Latitude (°)	Longitude (°)
Baoding urbs	S1	4	12	38.539403	115.276454
	S2	4	12	38.526999	115.300526
	S3	4	12	38.514755	115.31873
	S4	4	12	38.51369	115.300516
	S5	5	12	38.51043	115.27712
Baoding suburbs	S6	5	15	39.019777	115.182851
	S7	3	15	39.00263	115.250861
	S8	4	15	38.541516	115.226307
	S9	4	15	38.532176	115.312829
Baoding rural mountains	S10	5	30	39.077806	115.111414
	S11	5	30	39.077451	115.11137
	S12	5	12	38.044153	114.280569
Shijiazhuang urbs	S13	4	12	38.041514	114.333161
	S14	4	12	38.023908	114.31005
	S15	3	12	38.01923	114.336841
	S16	4	12	38.018082	114.27733
Shijiazhuang suburbs	S17	4	15	38.008468	114.219345
	S18	4	15	37.5804	114.209248
	S19	5	15	37.575959	114.267252
	S20	4	15	37.54984	114.238708
	S21	4	20	37.536216	114.220331
Shijiazhuang rural mountains	S22	5	20	37.53165	114.219133
	S23	2	20	37.523087	114.219845
Total	23	95			

### Sample preparation and element determination

The procedures of sample preparation and element determination have been detailed in our previous studies (Li et al., 2024; Lin et al., 2024). In short, the recovered samples were cleaned, oven-dried, ground, homogenized, and mineralized using a HNO<sub>3</sub>-H<sub>2</sub>O<sub>2</sub> microwave digestion system. Concentrations were tested for 55 elements using ICP-MS (Agilent 7700X, Agilent Technologies, Tokyo, Japan). These elements are Ag, Al, As, B, Ba, Be, Bi, Ca, Cd, Co, Cr, Cs, Cu, Fe, Ge, Hg, K, Li, Mg, Mn, Mo, Na, Nb, Ni, P, Pb, Rb, S, Sb, Se, Si, Sn, Sr, Th, Ti, Tl, U, V, and Zn, as well as 16 REEs (Sc, Y, La, Ce, Pr, Nd, Sm, Eu, Gd, Tb, Dy, Ho, Er, Tm, Yb, and Lu). Reference materials for quality control purpose are GBW10014 (cabbage), GBW10015 (spinach) and GBW10052 (green tea; all from the Institute of Geophysical and Geochemical Exploration, Chinese Academy of Geological Sciences) and IAEA-336 (a Portugal lichen from International Atomic Energy Organization).

### EU ratio and the interpretive scale for lichen transplants

EU ratio was calculated using Eq. (1):

$$EU = \frac{[X]_{\text{exposed}}}{[X]_{\text{unexposed}}} \times 100 \quad (\text{Eq.1})$$

where [X] represents concentration of element X, the subscripts indicate which sample the concentration referred to.

We adopted the 12-week interpretive bioaccumulation scale (Cecconi et al., 2019) to evaluate the bioaccumulation level of elements in *RSI*. In this scale,  $EU \leq 1$  denotes absence of bioaccumulation;  $1 < EU \leq 1.8$  denotes low bioaccumulation;  $1.8 < EU \leq 3.1$  denotes moderate bioaccumulation;  $3.1 < EU \leq 3.7$  denotes high bioaccumulation; and  $EU > 3.7$  denotes severe bioaccumulation.

### Statistical analyses

Coefficient of variation (CV) were calculated using *Eq. (2)*:

$$CV = \frac{SD}{\text{Mean}} \times 100 \quad (\text{Eq.2})$$

where SD denotes standard deviation.

Data normality was tested using a Shapiro-Wilk test. Homogeneity of variances were tested using Leven's test. Concentration difference between exposure site and background area were tested using an independent samples T test.

The EU ratios were log-transformed to enhance data normality. A two-way analysis of variance (Two-way ANOVA) with a Turkey' HSD test for multiple comparisons was performed on the log-transformed EU ratios to test the main effects of cities and ecotopes and their interactions. A simple effect analysis was performed on data with significant interactive effects.

Each exposure site was weighted according to *Table 1* to ensure an equal number of exposure sites between exposure areas. Then a type-R cluster analysis was performed on the log-transformed EU ratios. A Ward's method was used for clustering on the Euclidean distance matrix.

Statistical analyses were performed using PAST 4.17C software (Ø. Hammer, June 2024). The other analyses were performed using SPSS 21.0 software (SPSS Inc., Chicago, IL, USA).

## Results

*Table 2* presents the unexposed concentrations of 55 elements in *RSI*. The unexposed concentrations are  $K > Si > Ca > Al > S > P > Fe > Mg > Na > Ti > Mn > Zn > Ba > Sr > B > Cu > Rb > Cr > Pb > V > Ce > Co > As > Ni > La > Li > Nd > Y > Se > Sc > Hg > Th > Pr > Sn > Cs > Sm > Ge > Gd > Mo > Nb > Dy > Cd > Sb > Bi > U > Er > Yb > Be > Tl > Ag > Eu > Ho > Tb > Tm > Lu$ . They have a high variability for Ca (CV = 38.4%), Co (66.2%) and Hg (36.0%), and a low variability for all the other elements (CV < 14.0%).

*Table 3* presents the exposed concentrations of 55 elements in six exposure areas. The element ranks of the exposed concentrations are roughly similar to that of the unexposed concentrations. In each exposure area, the exposed concentrations are significantly lower than the unexposed concentrations for K and P, are not different from the unexposed

concentrations for Ca, Co and Hg, but are significantly higher than the unexposed concentrations for all the other 50 elements.

**Table 2.** Unexposed concentrations ( $\mu\text{g}\cdot\text{g}^{-1}$ ) and their variability (CV%) of 55 elements in *Ramalina sinensis*.  $n = 5$  for each element

	Mean ( $\mu\text{g}\cdot\text{g}^{-1}$ )	CV (%)		Mean ( $\mu\text{g}\cdot\text{g}^{-1}$ )	CV (%)
Ag	0.032	9.37	Sb	0.075	8.84
Al	1389	6.55	Se	0.303	4.27
As	1.258	7.88	Si	4084	4.39
B	4.801	9.93	Sn	0.201	7.06
Ba	11.74	5.45	Sr	5.696	9.76
Be	0.036	8.73	Th	0.239	4.21
Bi	0.062	9.84	Ti	62.44	5.30
Ca	1463	38.41	Tl	0.034	11.31
Cd	0.081	9.59	U	0.060	3.20
Co	1.824	66.21	V	1.953	3.18
Cr	2.546	11.76	Zn	21.73	10.54
Cs	0.177	3.39			
Cu	3.911	9.37		Rare earth elements	
Fe	759.1	4.83	Sc	0.302	4.91
Ge	0.136	7.62	Y	0.530	4.18
Hg	0.281	35.98	La	0.938	3.58
K	4416	4.99	Ce	1.836	4.07
Li	0.848	6.33	Pr	0.206	4.43
Mg	509.6	8.87	Nd	0.792	4.74
Mn	24.67	8.14	Sm	0.144	4.86
Mo	0.121	9.31	Eu	0.032	3.85
Na	248.3	8.84	Gd	0.128	4.71
Nb	0.107	6.18	Tb	0.017	4.86
Ni	1.017	7.42	Dy	0.099	5.05
P	918.6	13.07	Ho	0.019	5.10
Pb	2.009	7.19	Er	0.052	5.73
Rb	3.272	8.67	Tm	0.007	4.57
S	935.6	13.10	Yb	0.046	4.28
			Lu	0.006	5.23

*Fig. 2a* presents the results of type-R cluster analysis (Ward's method, Euclidean distance) performed on the log-transformed EU ratios of 50 elements (all elements barring Ca, Co, Hg, K, and P) at 23 exposure sites, with each site being weighted according to *Table 1*. The elements are divided into 3 groups (Cophenetic correlation = 0.75; *Fig. 2a*). The group G1 consists of Cr and Sb. The group G2 consists of 42 elements (Ag, Al, Ba, Be, Bi, Cd, Cs, Cu, Fe, Li, Mn, Mo, Na, Nb, Ni, Pb, Rb, S, Si, Sn, Sr, Th, Ti, Tl, U, V, and 16 REEs). The group G3 consists of 6 elements (As, B, Ge, Mg, Se, and Zn).

*Fig. 2b* presents the results of Two-way ANOVA (city  $\times$  ecotope) performed on the unweighted log-transformed EU ratios of 50 elements in 95 samples. The exposed concentrations were not different between Baoding and Shijiazhuang for all of the 50 elements except B and Be, and not different among ecotopes for all of the 50 elements except Al, B, Ba, Sb, Si, and Sn. The exposed concentrations of Al and Si are generally higher in the suburbs than in the urbs. The exposed concentrations of Ba, Sb, and Sn are lower in the rural mountains than in the urbs and suburbs.

**Table 3.** Exposed concentrations ( $\mu\text{g}\cdot\text{g}^{-1}$ ) of 55 elements in *Ramalina sinensis* in three ecotopes of Baoding and Shijiazhuang

	Baoding			Shijiazhuang		
	Urbs (n = 5)	Suburbs (n = 4)	Rural mountains (n = 2)	Urbs (n = 5)	Suburbs (n = 4)	Rural mountains (n = 3)
Ag	0.047 (0.004)	0.049 (0.003)	0.049 (0.004)	0.047 (0.002)	0.044 (0.003)	0.051 (0.006)
Al	2005 (211.2)	2502 (472.2)	2479 (506.5)	2025 (191.7)	2326 (76.88)	1959 (54.04)
As	1.807 (0.117)	1.703 (0.071)	1.611 (0.144)	1.725 (0.068)	1.683 (0.093)	1.656 (0.133)
B	6.026 (0.337)	6.442 (1.305)	6.618 (0.781)	8.072 (0.860)	7.780 (0.673)	5.833 (0.344)
Ba	17.62 (1.107)	20.30 (1.055)	17.93 (1.986)	18.00 (1.903)	19.05 (1.410)	17.12 (1.130)
Be	0.051 (0.004)	0.056 (0.008)	0.058 (0.009)	0.064 (0.005)	0.063 (0.007)	0.055 (0.004)
Bi	0.101 (0.009)	0.100 (0.016)	0.094 (0.009)	0.095 (0.005)	0.104 (0.003)	0.099 (0.009)
Ca	2089 (308.4) !	2268 (460.3) !	2237 (648.8) !	3063 (874.3)	2793 (1178) !	2548 (908.2) !
Cd	0.124 (0.008)	0.120 (0.017)	0.127 (0.011)	0.126 (0.008)	0.131 (0.025)	0.131 (0.017)
Co	1.497 (1.491) !	3.296 (2.043) !	1.936 (0.321) !	1.848 (0.803) !	2.167 (0.861) !	1.722 (0.395) !
Cr	5.157 (0.703)	5.560 (0.983)	5.129 (0.498)	5.278 (0.409)	5.499 (0.427)	6.308 (0.268)
Cs	0.268 (0.021)	0.290 (0.028)	0.290 (0.040)	0.277 (0.021)	0.297 (0.006)	0.285 (0.026)
Cu	6.058 (0.211)	5.808 (0.368)	5.585 (0.297)	6.013 (0.177)	5.940 (0.744)	5.779 (0.369)
Fe	1154 (90.82)	1244 (176.8)	1161 (170.5)	1295 (92.00)	1309 (120.0)	1208 (98.31)
Ge	0.177 (0.015)	0.188 (0.019)	0.177 (0.019)	0.181 (0.012)	0.193 (0.003)	0.185 (0.016)
Hg	0.267 (0.042) !	0.288 (0.054) !	0.351 (0.026) !	0.299 (0.074) !	0.360 (0.100) !	0.363 (0.041) !
K	3409 (107.8) #	3300 (182.1) #	3025 (207.0) #	3571 (97.55) #	3288 (385.1) #	3260 (102.8) #
Li	1.328 (0.097)	1.450 (0.205)	1.324 (0.191)	1.374 (0.101)	1.476 (0.102)	1.377 (0.097)
Mg	742.3 (32.85)	784.3 (105.0)	652.7 (73.16)	772.4 (52.06)	735.0 (121.1)	683.1 (27.78)
Mn	40.16 (2.076)	42.29 (4.653)	39.15 (2.386)	43.13 (1.365)	42.86 (5.846)	40.86 (1.084)
Mo	0.188 (0.008)	0.194 (0.015)	0.184 (0.009)	0.202 (0.014)	0.198 (0.012)	0.185 (0.017)
Na	393.2 (36.86)	372.0 (55.93)	314.1 (23.82)	409.9 (33.85)	438.0 (144.4)	348.4 (6.680)
Nb	0.165 (0.011)	0.174 (0.017)	0.173 (0.014)	0.177 (0.010)	0.180 (0.010)	0.168 (0.011)
Ni	1.711 (0.134)	1.767 (0.219)	1.632 (0.198)	1.722 (0.114)	1.797 (0.096)	1.767 (0.114)
P	811.6 (39.27) #	763.6 (63.15) #	737.7 (48.34) #	646.4 (18.13) #	694.0 (51.43) #	812.1 (79.29) #
Pb	3.244 (0.231)	3.106 (0.455)	2.990 (0.586)	2.974 (0.322)	3.177 (0.435)	3.107 (0.462)
Rb	4.958 (0.379)	5.199 (0.515)	4.931 (0.410)	5.038 (0.354)	5.045 (0.368)	5.104 (0.170)
S	1515 (67.42)	1545 (161.8)	1225 (87.30)	1526 (11.64)	1633 (372.2)	1445 (102.0)
Sb	0.160 (0.012)	0.150 (0.030)	0.127 (0.011)	0.135 (0.013)	0.139 (0.016)	0.118 (0.004)
Se	0.354 (0.021)	0.375 (0.030)	0.371 (0.032)	0.381 (0.013)	0.387 (0.024)	0.372 (0.032)
Si	5434 (435.2)	7041 (1211)	6811 (988.9)	6034 (523.4)	6254 (207.1)	5690 (223.7)
Sn	0.337 (0.025)	0.314 (0.028)	0.292 (0.018)	0.324 (0.026)	0.313 (0.009)	0.289 (0.022)
Sr	8.166 (0.800)	8.718 (1.189)	8.487 (1.538)	9.346 (1.454)	9.228 (1.767)	8.617 (1.277)
Th	0.369 (0.033)	0.403 (0.051)	0.383 (0.046)	0.388 (0.029)	0.418 (0.017)	0.391 (0.025)
Ti	90.21 (6.507)	93.57 (10.37)	88.62 (9.716)	99.06 (6.005)	97.26 (7.492)	89.58 (6.561)
Tl	0.046 (0.004)	0.051 (0.006)	0.052 (0.009)	0.048 (0.003)	0.056 (0.004)	0.052 (0.008)
U	0.089 (0.008)	0.097 (0.011)	0.095 (0.012)	0.095 (0.008)	0.099 (0.004)	0.094 (0.006)
V	3.017 (0.253)	3.196 (0.465)	2.919 (0.422)	3.172 (0.223)	3.273 (0.241)	3.083 (0.285)
Zn	31.10 (1.089)	29.31 (1.553)	28.71 (1.838)	31.07 (1.400)	31.69 (4.426)	28.95 (1.295)
Rare earth elements						
Sc	0.455 (0.038)	0.484 (0.064)	0.444 (0.060)	0.498 (0.031)	0.500 (0.043)	0.469 (0.044)
Y	0.783 (0.061)	0.844 (0.084)	0.846 (0.102)	0.848 (0.069)	0.870 (0.067)	0.819 (0.079)
La	1.409 (0.124)	1.531 (0.156)	1.527 (0.194)	1.497 (0.133)	1.581 (0.074)	1.489 (0.129)
Ce	2.785 (0.250)	3.057 (0.343)	3.013 (0.398)	2.932 (0.270)	3.141 (0.143)	2.962 (0.260)
Pr	0.310 (0.026)	0.341 (0.036)	0.344 (0.044)	0.329 (0.030)	0.350 (0.015)	0.330 (0.027)
Nd	1.183 (0.102)	1.306 (0.139)	1.313 (0.172)	1.274 (0.116)	1.347 (0.065)	1.267 (0.109)
Sm	0.216 (0.018)	0.235 (0.025)	0.233 (0.031)	0.235 (0.020)	0.242 (0.015)	0.230 (0.021)
Eu	0.048 (0.004)	0.051 (0.005)	0.050 (0.007)	0.050 (0.004)	0.053 (0.003)	0.050 (0.005)
Gd	0.192 (0.015)	0.207 (0.022)	0.202 (0.027)	0.206 (0.018)	0.214 (0.014)	0.204 (0.019)

	Baoding			Shijiazhuang		
	Urbs (n = 5)	Suburbs (n = 4)	Rural mountains (n = 2)	Urbs (n = 5)	Suburbs (n = 4)	Rural mountains (n = 3)
Tb	0.026 (0.002)	0.028 (0.003)	0.028 (0.004)	0.028 (0.002)	0.029 (0.002)	0.028 (0.002)
Dy	0.149 (0.011)	0.161 (0.016)	0.159 (0.019)	0.160 (0.013)	0.166 (0.011)	0.158 (0.014)
Ho	0.028 (0.002)	0.030 (0.003)	0.030 (0.004)	0.030 (0.002)	0.031 (0.002)	0.030 (0.003)
Er	0.078 (0.006)	0.084 (0.009)	0.084 (0.010)	0.085 (0.007)	0.087 (0.006)	0.083 (0.007)
Tm	0.011 (0.001)	0.012 (0.001)	0.012 (0.001)	0.012 (0.001)	0.012 (0.001)	0.012 (0.001)
Yb	0.070 (0.006)	0.075 (0.008)	0.074 (0.009)	0.074 (0.005)	0.077 (0.005)	0.073 (0.006)
Lu	0.010 (0.001)	0.010 (0.001)	0.011 (0.001)	0.011 (0.001)	0.011 (0.001)	0.010 (0.001)

Values are mean with a standard deviation in bracket. A “!” and a “#” following concentrations indicates that the exposed concentrations were similar to and lower than the unexposed concentrations, respectively. The concentrations without any marks were higher than the unexposed concentrations

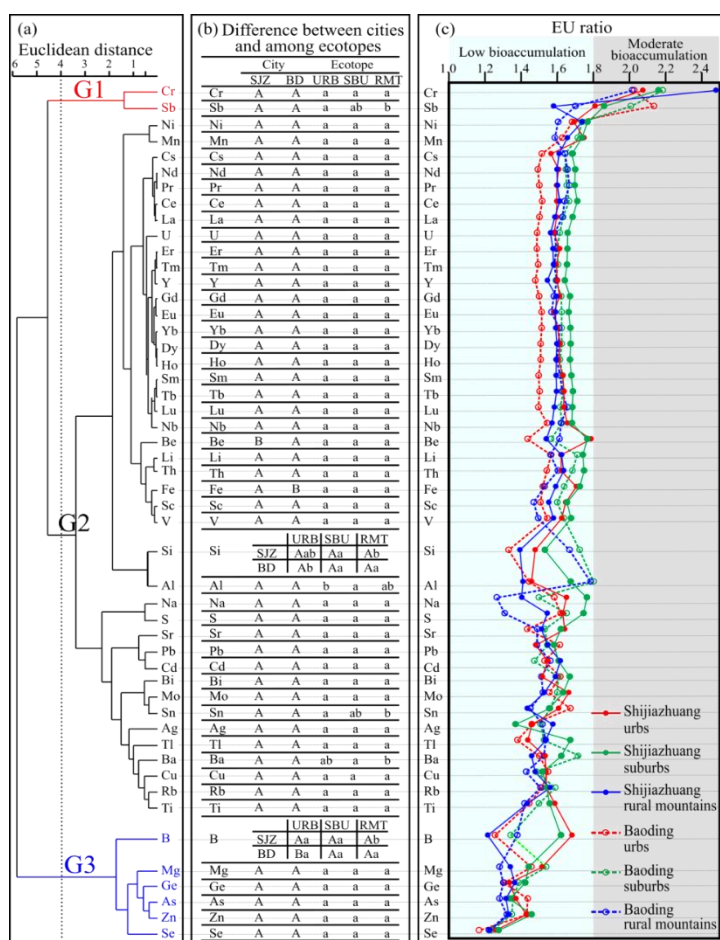


**Figure 2.** a. Cluster diagram using Ward’s method on Euclidean distance matrix of exposed to unexposed ratios (EU) of 50 elements in *Ramalina sinensis*. EU ratios were log-transformed after weighting according to Table 1. b. Differences between cities and among ecotopes. Different capital letters and small letters indicate a significant difference between cities and among ecotopes, respectively. Significance was tested using Two-way ANOVA with Tukey test for multiple comparison. A simple effect test was performed for elements (Si and B) with a significance interactive effects between the cities and among the ecotopes. SJZ denotes Shijiazhuang, BD denotes Baoding, URB denotes urbs. SBU denotes suburbs. RMT denotes rural mountains. c. EU ratios for 50 elements in *Ramalina sinensis* from six exposure areas (2 cities × 3 ecotopes)

*Fig. 2c* presents the mean EU ratios for each of the six exposure areas. Bioaccumulation of Cr is of moderate bioaccumulation in all exposure areas. Bioaccumulation of Sb is of moderate bioaccumulation in urbs and suburbs, and of low bioaccumulation in rural mountains. Bioaccumulation for the other 48 elements are of low bioaccumulation in all exposure areas.

## Discussions

### *Element bioaccumulation and loss*

Five elements (Ca, Co, Hg, K, and P; *Table 3*) were not accumulated in *RSI* after being exposed for 140 days. Theoretically, the exposed concentrations of Ca, K, and P could be higher than the unexposed concentrations, at least in urbs and suburbs. This is because these elements are rock-forming elements and therefore dominant components in the atmospheric particulates of crustal origin. However, exposed concentrations of K and P are significantly lower than the unexposed concentrations in all of the six exposure areas, indicating nutrient loss from thalli of *RSI* during exposure. Loss of nutrients are often associated with decrease in lichen metabolic activities (Cecconi et al., 2018), and both are strongly affected by air pollution and climate changes (Vannini et al., 2017; Cecconi et al., 2021; Bajpai et al., 2022; Kováčik et al., 2023; Kumari et al., 2024). The relevant studies have also observed that the trends of K and P in lichens is different from or even opposite to those of the pollutants (Adams et al., 2012; Yemets et al., 2014; Gao et al., 2021). Li et al. (2024) pointed out that the use of *RSI* as an active biomonitor can greatly underestimate the atmospheric deposition of K and P.

The 0 bioaccumulation of Ca, Co and Hg in *RSI* might be attributable to the great heterogeneity in the unexposed concentrations (CV: 36.0~66.2%; *Table 2*). The relevant studies suggest that the local variation in the background concentrations should be controlled to  $\leq 25\%$  (Malaspina et al., 2014; Chahloul et al., 2022; Zheng et al., 2023), otherwise may lead to an inflated false negative rate in comparing element concentrations before and after exposure. We have adopted measures to minimize the heterogeneity of unexposed concentrations, such as the thallus size, and bark aspect and height in sample collection, and the use of composite sample after water washing. Although these measures are popular and effective (Agnan et al., 2014; Klos et al., 2018; Dörter et al., 2020; Zheng et al., 2023), we failed to control variability of unexposed concentrations for the three element to an acceptable level.

The other 50 elements are bioaccumulated in *RSI*, with the exposed concentrations higher than the unexposed concentrations in all of the six exposure areas (*Table 3*). This trend matches the fact that the exposure areas had higher air pollutant concentrations than the background area during exposure (*Fig. 1e*). This trend has also been found in active biomonitoring studies using *RSI* in the cities of Iran and Northern China (Tumur et al., 2011; Sohrabi et al., 2021; Gao et al., 2022; Li et al., 2024).

### *Element sources and bioaccumulation level*

The G1 elements (Cr and Sb) were most likely derived from the industrial and traffic activities and had higher bioaccumulation levels (moderate bioaccumulation) than the other 48 elements (low bioaccumulation; *Fig. 2c*). Sb is a typical tracer of traffic emissions (Vannini et al., 2019). It had higher exposed concentrations in the urbs than in the rural mountains. These results are in line with the denser road network supporting heavier traffic

in the urbs than in the rural mountains of the two cities (*Fig. 1c,d*). Cr is a typical industrial element in northern China (Duan et al., 2013). The exposed concentrations of both Cr and Sb were similar between the urbs and suburbs and between the two cities, in line with the spatial patterns in PM<sub>10</sub> and PM<sub>2.5</sub> concentrations (*Fig. 1e*). These results highlight the importance of industrial and traffic emissions to air quality of Baoding and Shijiazhuang.

The G2 elements were from multiple sources, including traffic, industrial and domestic activities, as well as particulate matters of crustal origin. Sn and Mo have been regarded as tracers of traffic emissions (Lucadamo et al., 2016). The exposed concentrations of Sn were higher in the urbs than in rural mountains (*Fig. 2b*). This spatial pattern is the same as that of Sb, again highlighting the relative importance of traffic emissions to air quality. S is a main pollutant in the haze of North China Plain (Wang et al., 2018) and can be released in a large amount by industrial and domestic activities using coal as fuel in winter heating period (Tian et al., 2015). In 2016, the atmospheric deposition of Cd and Pb in Shijiazhuang urbs were from power plants and traffic, and that of Cu came from traffic (Cai et al., 2019). In addition, Al, Sc, Fe, Ti, and 16 REEs have been regarded as of crustal origin and used as environmental tracers in most relevant studies (Agnan et al., 2014; Ratier et al., 2018; Dołęgowska et al., 2021). Therefore, crustal origin in the form of windblown dust is also an important source of the G2 elements accumulated in *RSI*.

The G3 elements (As, B, Ge, Mg, Se, and Zn), like G2 elements, were also from multiple sources. However, the G3 elements were more affected by lichen physiology than G2 elements. The atmospheric deposition of Zn in Shijiazhuang urbs in 2016 were from industrial and traffic activities (Cai et al., 2019). An active biomonitoring study in Tangshan city indicate that Mg and Zn accumulated in *RSI* were of atmospheric origin, Ge of crustal origin, and As and Se of crustal-atmospheric origin (Li et al., 2024). In addition, B, Mg, Se and Zn are nutrient elements. These nutrients can be accumulated in lichen thalli and can also be leached out from the lichens by rainwater.

Bioaccumulations of the G2 and G3 elements were of low bioaccumulation (*Fig. 2c*) and were similar between cities and among ecotopes (*Fig. 2b*). These results indicate that air pollution in the two cities during exposure period is low and dominated by the non-point pollution sources. This is obviously a result of the strict regulatory measures since 2013 to alleviate and control air pollution in China. Meteorological data show that, in the urban agglomeration of the North China Plain during 2014 to 2019, the number of "blue sky" days increased year by year, while the inverse occurred for the number and duration of persistent regional pollution events and the concentration of atmospheric suspended particles (Li et al., 2020). However, the release of Cr and Sb deserves further attention.

## Conclusions

Exposed concentrations were higher than unexposed concentrations for 50 elements, indicating that *Ramalina sinensis* is a good active biomonitor for atmospheric deposition of these metal/metalloids. Exposed concentrations of K and P were low than unexposed concentrations, indicating a negative effect of air pollution on lichen physiology. Cr and Sb were of moderate bioaccumulation, indicating that the industrial and traffic activities were important sources of air pollution. The other 48 elements were of low bioaccumulation and had similar concentrations between cities and among ecotopes, indicating a low air pollution dominated by various non-point sources.

**Declaration of competing interest.** The authors declare no conflicts of interest.

**Acknowledgments.** The authors would like to thank the National Natural Science Foundation of China (grant number 32471780) and the Natural Science Foundation of Hebei Province (grant number D2020201002) for their financial supports.

## REFERENCES

- [1] Abas, A. (2021): A systematic review on biomonitoring using lichen as the biological indicator: A decade of practices, progress and challenges. – *Ecological Indicators* 121: 107197.
- [2] Adams, M. D., Gottardo, C. (2012): Measuring lichen specimen characteristics to reduce relative local uncertainties for trace element biomonitoring. – *Atmospheric Pollution Research* 3: 325-330.
- [3] Agnan, Y., Séjalondelmas, N., Probst, A. (2014): Origin and distribution of rare earth elements in various lichen and moss species over the last century in France. – *Science of The Total Environment* 487: 1-12.
- [4] Bajpai, R., Shukla, V., Raju, A., Singh, C. P., Upreti, D. K. (2022): A geostatistical approach to compare metal accumulation pattern by lichens in plain and mountainous regions of northern and central India. – *Environmental Earth Sciences* 81: 203.
- [5] Brunialti, G., Frati, L. (2014): Bioaccumulation with lichens: The Italian experience. – *International Journal of Environmental Studies* 71: 15-26.
- [6] Cai, K., Li, C., Na, S. (2019): Spatial Distribution, Pollution Source, and Health Risk Assessment of Heavy Metals in Atmospheric Depositions: A Case Study from the Sustainable City of Shijiazhuang, China. – *Atmosphere* 10: 222.
- [7] Cecconi, E., Incerti, G., Capozzi, F., Adamo, P., Bargagli, R., Benesperi, R., Carniel, F. C., Favero-Longo, S. E., Giordano, S., Puntillo, D., Ravera, S., Spagnuolo, V., Tretiach, M. (2018): Background element content of the lichen *Pseudevernia furfuracea*: A supra-national state of art implemented by novel field data from Italy. – *Science of The Total Environment* 622/623: 282-292.
- [8] Cecconi, E., Fortuna, L., Benesperi, R., Bianchi, E., Brunialti, G., Contardo, T., Di Nuzzo, L., Frati, L., Monaci, F., Munzi, S., Nascimbene, J., Paoli, L., Ravera, S., Vannini, A., Giordani, P., Loppi, S., Tretiach, M. (2019): New interpretative scales for lichen bioaccumulation data: The Italian proposal. – *Atmosphere* 10: 136.
- [9] Cecconi, E., Fortuna, L., Peplis, M., Mauro, T. (2021): Element accumulation performance of living and dead lichens in a large-scale transplant application. – *Environmental Science and Pollution Research* 28: 16214-16226.
- [10] Chahloul, N., Khadhri, A., Vannini, A., Mendili, M., Raies, A., Loppi, S. (2022): Bioaccumulation of potentially toxic elements in some lichen species from two remote sites of Tunisia. – *Biologia* 77: 2469-2473.
- [11] Dołęgowska, S., Gałuszka, A., Migaszewski, Z. M. (2021): Significance of the long-term biomonitoring studies for understanding the impact of pollutants on the environment based on a synthesis of 25-year biomonitoring in the Holy Cross Mountains, Poland. – *Environmental Science and Pollution Research* 28: 10413-10435.
- [12] Dörter, M., Karadeniz, H., Saklangıç, U., Yenisoy-Karakaş, S. (2020): The use of passive lichen biomonitoring in combination with positive matrix factor analysis and stable isotopic ratios to assess the metal pollution sources in throughfall deposition of Bolu plain, Turkey. – *Ecological Indicators* 113: 106212.
- [13] Duan, J. C., Tan, J. H. (2013): Atmospheric heavy metals and Arsenic in China: Situation, sources and control policies. – *Atmospheric Environment* 74: 93-101.
- [14] Gao, J., Wu, Y.-Y., Liu, B.-Y., Zhao, R.-K., Liu, A.-Q., Li, X., Chen, Q.-Z., Sun, L.-W., Guo, X.-P., Liu, H.-J. (2021): Vertical distribution patterns of element concentrations in

- podetia of *Cladonia rangiferina* from Huzhong Natural Reserve, Heilongjiang, China. – Polish Journal of Environmental Studies 30: 103-110.
- [15] Gao, J., Zhang, L. Y., Li, X., Ma, C. P., Jin, Q., Liu, L., Zhang, J. M., Zhao, L. C., Meng, J. W., Liu, H. J. (2022): Effects of canopy and exposure duration on element composition of the transplanted lichen *Ramalina sinensis*. – Chinese Journal of Ecology 41: 2289-2298.
- [16] Godinho, R. M., Wolterbeek, H. T., Pinheiro, M. T., Alves, L. C., Verburg, T. G., Freitas, M. C. (2009): Micro-scale elemental distribution in the thallus of *Flavoparmelia caperata* transplanted to polluted site. – Journal of Radioanalytical and Nuclear Chemistry 281: 205-210.
- [17] Jia, S. J., Zhang, X., Liu, Q. X., Chen, Q. Z., Li, X., Pang, X. M., Li, J. J., Wu, Q. F., Zhao, L. C., Liu, H. J. (2020): Spatial-temporal patterns of element concentrations in *Xanthoparmelia camtschadalis* transplanted along roads. – Polish Journal of Environmental Studies 29: 121-129.
- [18] Klos, A., Ziembik, Z., Rajfur, M., Dolhanczuk-Srodka, A., Bochenek, Z., Bjerke, J. W., Tommervik, H., Zagajewski, B., Ziolkowski, D., Jerz, D., Zielinska, M., Krems, P., Godyn, P., Marciniak, M., Swislawski, P. (2018): Using moss and lichens in biomonitoring of heavy-metal contamination of forest areas in southern and north-eastern Poland. – Sci Total Environ 627: 438-449.
- [19] Kováčik, J., Husáková, L., Vlása, M., Piroutková, M., Vydra, M., Patočka, J., Filip, M. (2023): Elemental profile identifies metallurgical pollution in epiphytic lichen *Xanthoria parietina* and (hypo)xanthine correlates with metals. – Science of The Total Environment 883: 163527.
- [20] Kumari, K., Kumar, V., Nayaka, S., Saxena, G., Sanyal, I. (2024): Physiological alterations and heavy metal accumulation in the transplanted lichen *Pyxine cocolos* (Sw.) Nyl. in Lucknow city, Uttar Pradesh. – Environmental Monitoring and Assessment 196: 84.
- [21] Li, M. G., Wang, L. L., Liu, J. D., Gao, W. K., Song, T., Sun, Y., Li, L., Li, X. R., Wang, Y. H., Liu, L. L., Daellenbach, K. R., Paasonen, P. J., Kerminen, V.-M., Kulmala, M., Wang, Y. S. (2020): Exploring the regional pollution characteristics and meteorological formation mechanism of PM<sub>2.5</sub> in North China during 2013-2017. – Environment International 134: 105283.
- [22] Li, M. N., Meng, J. W., Lin, D., Xu, P., Wang, L., Hu, Y. Q., Qin, C., Zhao, L. C., Xia, Y., Zhang, L. Y., Liu, H. J. (2024): Active biomonitoring of atmospheric element deposition in the heating period of Tangshan using *Ramalina sinensis*. – Polish Journal of Environmental Studies 33: 5767-5778.
- [23] Lin, D., Meng, J. W., Li, M. N., Wu, Q. F., Wang, L. P., Li, X. J., Song, J. J., Zhao, L. C., Xu, P., Xia, Y., Liu, H. J. (2024): Active biomonitoring of atmospheric element deposition using *Evernia mesomorpha* in Tangshan, China. – Applied Ecology and Environmental Research 22: 1191-1205.
- [24] Lucadamo, L., Corapi, A., Loppi, S., De Rosa, R., Barca, D., Vespasiano, G., Gallo, L. (2016): Spatial variation in the accumulation of elements in thalli of the lichen *Pseudevernia furfuracea* (L.) Zopf transplanted around a biomass power plant in Italy. – Archives of Environmental Contamination and Toxicology 70: 506-521.
- [25] Malaspina, P., Giordani, P., Modenesi, P., Abemoschi, M. L., Magi, E., Soggia, F. (2014): Bioaccumulation capacity of two chemical varieties of the lichen *Pseudevernia furfuracea*. – Ecological Indicators 45: 605-610.
- [26] Massimi, L., Conti, M. E., Mele, G., Ristorini, M., Astolfi, M. L., Canepari, S. (2019): Lichen transplants as indicators of atmospheric element concentrations: a high spatial resolution comparison with PM<sub>10</sub> samples in a polluted area (Central Italy). – Ecological Indicators 101: 759-769.
- [27] Paoli, L., Vannini, A., Fačková, Z., Guarnieri, M., Bačkor, M., Loppi, S. (2018): One year of transplant: Is it enough for lichens to reflect the new atmospheric conditions? – Ecological Indicators 88: 495-502.

- [28] Peng, H., Chen, Y., Weng, L., Ma, J., Ma, Y., Li, Y., Islam, M. S. (2019): Comparisons of heavy metal input inventory in agricultural soils in North and South China: A review. – *Science of The Total Environment* 660: 776-786.
- [29] Ratier, A., Dron, J., Revenko, G., Austruy, A., Dauphin, C.-E., Chaspoul, F., Wafo, E. (2018): Characterization of atmospheric emission sources in lichen from metal and organic contaminant patterns. – *Environmental Science and Pollution Research* 25: 8364-8376.
- [30] Sohrabi, M., Hassanzadeh, N., Hedayatzadeh, F., Mofid, M. (2021): Air quality and trace elements biomonitoring in Tehran urban areas using epiphytic lichen. – *Iranian Journal of Health and Environment* 13: 705-734.
- [31] Tian, H. Z., Zhu, C. Y., Gao, J. J., Cheng, K., Hao, J. M., Wang, K., Hua, S. B., Wang, Y., Zhou, J. R. (2015): Quantitative assessment of atmospheric emissions of toxic heavy metals from anthropogenic sources in China: historical trend, spatial distribution, uncertainties and control policies. – *Atmospheric Chemistry and Physics* 15: 10127-10147.
- [32] Tumor, A., Abdulla, A., Abbas, A. (2011): Bio-monitoring of air quality in Urumqi city using lichens transplant method. – *Environmental Pollution and Control* 33: 1-8.
- [33] Vannini, A., Paoli, L., Nicolardi, V., Di Lella, L. A., Loppi, S. (2017): Seasonal variations in intracellular trace element content and physiological parameters in the lichen *Evernia prunastri* transplanted to an urban environment. – *Acta Botanica Croatica* 76: 171-176.
- [34] Vannini, A., Paoli, L., Russo, A., Loppi, S. (2019): Contribution of submicronic (PM<sub>1</sub>) and coarse (PM<sub>>1</sub>) particulate matter deposition to the heavy metal load of lichens transplanted along a busy road. – *Chemosphere* 231: 121-125.
- [35] Wang, L. L., Li, W. J., Sun, Y., Tao, M. H., Xin, J. Y., Song, T., Li, X. R., Zhang, N., Ying, K., Wang, Y. S. (2018): PM<sub>2.5</sub> characteristics and regional transport contribution in five cities in southern North China Plain, during 2013-2015. – *Atmosphere* 9: 157.
- [36] Wang, Y. S., Li, W. J., Gao, W. K., Liu, Z. R., Tian, S. L., Shen, R. R., Ji, D. S., Wang, S., Wang, L. L., Tang, G. Q., Song, T., Chen, M. T., Wang, G. H., Gong, Z. Y., Hao, J. M., Zhang, Y. H. (2019): Trends in particulate matter and its chemical compositions in China from 2013-2017. – *Science China Earth Sciences* 62: 1857-1871.
- [37] Yemets, O. A., Solhaug, K. A., Gauslaa, Y. (2014): Spatial dispersal of airborne pollutants and their effects on growth and viability of lichen transplants along a rural highway in Norway. – *Lichenologist* 46: 809-823.
- [38] Zhao, L. L., Zhang, C., Jia, S. J., Liu, Q. X., Chen, Q. Z., Li, X., Liu, X. D., Wu, Q. F., Zhao, L. C., Liu, H. J. (2019): Element bioaccumulation in lichens transplanted along two roads: The source and integration time of elements. – *Ecological Indicators* 99: 101-107.
- [39] Zheng, X., Wu, Q. F., Wang, L. P., Liu, A. Q., Xu, C. Y., Li, X. J., Zhao, L. C., Xu, D., Meng, J. W., Liu, H. J. (2023): Composite samples with a small sample size reflect mean element concentrations in three lichens differing in element-specific concentrations. – *Applied Ecology and Environmental Research* 21: 609-622.